Type: Methods Paper

Title: Electroretinograms as a functional readout of neuronal integrity in neurodegeneration models of *Drosophila melanogaster*

Author names and affiliations: **Nikhil Manuel[1], **Malav Mallipudi[2,4], **Arya Gajwani[1], Sravan Gopalkrishna Shetty Sreenivasa Murthy[2,3], Daniel C. Jupiter[5], Balaji Krishnan[1,2,3]

** Authors contributed equally to the work

[1] – John Sealy School of Medicine, University of Texas Medical Branch at Galveston

[2] – Department of Neurology, University of Texas Medical Branch

[3] – Mitchell Center for Neurodegenerative Diseases, University of Texas Medical Branch

[4] – School of Behavioral and Brain Sciences, University of Texas at Dallas

[5] – Department of Biostatistics and Data Science, University of Texas Medical Branch

Corresponding Author:

Balaji Krishnan, PhD
Associate Professor,
Don and Nancy Mafrige Professor of Neurodegenerative Research in the honor of Dr. Brent Masel, MD.
Department of Neurology, Mitchell Center for Neurodegenerative Diseases,
301 University Blvd., Galveston, TX 77555-1045, U.S.A.
Phone : (409) 772-8069
Fax : (409) 747-0015
E-mail : bakrishn@utmb.edu

Highlights: Highlights should be submitted in a separate editable file in the online submission system. Please use 'Highlights' in the file name and include 3 to 5 bullet points (maximum 85 characters, including spaces, per bullet point)

- *Drosophila* ommatidia as a functional measure of neuronal integrity
- GAL4-UAS neurogenetics to study neurodegenerative states
- Healthy and pathological aging assessments
- An insight into characteristics of disease model ERGs

Abstract

The current protocol leverages the intrinsic potential of electroretinograms (ERGs) in *Drosophila melanogaster*, extending their application by using aged flies and the GAL4-UAS system to attempt to understand human gene effects on neuronal transmission. ERGs model neuronal vulnerability and developmental changes, providing a robust tool for examining altered neurological states. The current protocols sheds insights into the strengths and pitfalls in the analysis of human gene pathways in progression of neurodegenerative states, with additional information on novel parameters that can be tapped. This technique enhances our ability to use neurophysiological recordings for gaining insights into the molecular mechanisms underlying the role of the gene in neuronal function, thus complementing ex vivo and in vitro systems using mouse and cell culture models.

- Genetics and aging to studying neurodegeneration
- Traditional ERG parameters
- Additional parameters

Our technique builds on the robust background of several techniques to provide additional parameters such as aging the flies (1-5 weeks) and the response characteristics associated with creating transgenic models using the w^{1118} background. Lastly, we also provide a different way to explore the results by identifying zones and derivatives that may improve our electrophysiological of the genetic influences on neuronal responses better.

Graphical Abstract:

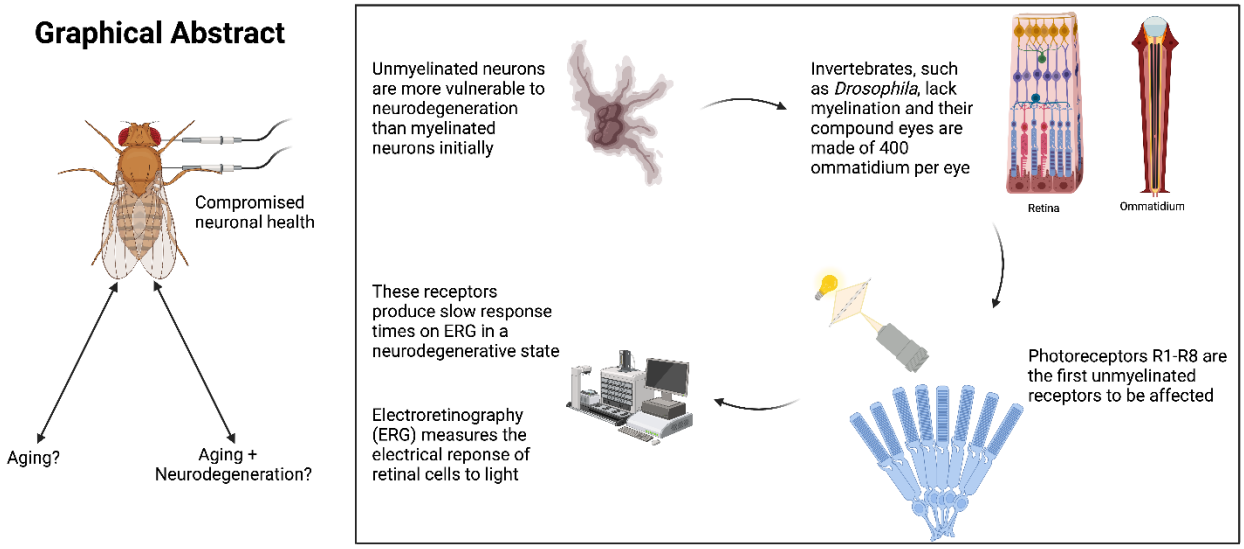

Keywords:

- ERG
- Neurodegeneration
- Aging
- w^{1118}
- CS
- GAL4-UAS

Abbreviations:
GAL4/UAS, GAL4/Upstream Activating Sequence; AD, Alzheimer's Disease; BDSC, Bloomington Drosophila Stock Center; APP, Amyloid Precursor Protein; APPL, Amyloid Precursor protein Homolog; MAPT, Microtubule-Associated Protein Tau; BACE1, beta-site amyloid precursor protein cleaving enzyme 1; ERG, Electroretinogram; Elav GAL4, Embryonic Lethal Abnormal Vision GAL4; w^{1118}, *white* 1118 PLD1, Phospholipase D Isoform 1; RPA, Receptor Potential Amplitude; CS, Canton S.

Funding Sources: This work was supported by research grants from the NIH R01 AG063945(B.K.), NIH R21 AG059223(B.K.), AARG-17-533363(B.K), The Don and Nancy Mafrige Professor in Neurodegenerative Disease Endowment (B.K.), Mitchell Center for Neurodegenerative Diseases (B.K.).

Ethics Statement: This study was conducted in accordance and compliance with the National Institutes of Health Guidelines: D4 for Animal/Arthropod Species: *Drosophila melanogaster* and approved by the Institutional Biosafety Committee (IBS) at UTMB under the Notification of Use (NOU: 2022128)" at the University of Texas Medical Branch (UTMB)

Method Details:

Scientific Premise:

ERGs are measured in immobilized living fruit flies, which can tolerate extended periods of anoxia without changes in the ERG. This allows for it to be possible to take stable measurements for many hours or even days under high humidity, where ERG signals are typically recorded with glass micropipettes having physiological saline (0.9% NaCl and chloridized wires). These yield resistances from a few kΩ to a few MΩ. The signal is amplified unipolarly in DC mode, with the recording electrode contacting the compound eye or inserted just below the cornea. The grounded reference electrode is placed in a non-illuminated part of the body (typically interior to thorax). The stimulus for obtaining an ERG is typically a simple light pulse lasting between 10 ms and 10 s. Suitable light sources include DC-operated halogen lamps, xenon arc lamps, or LEDs, but should not have flickering components at 50 Hz or 100 Hz, which the fly eye perceives as flicker, causing signal oscillations. To cover the entire dynamic working range of the *Drosophila* ERG, the light intensity needs to be adjusted over a range of 6 orders of magnitude, in steps no larger than 0.5 log units.

Due to the low lateral resistance between the ommatidia (the facets that make up the *Drosophila* compound eye) ERG is not a localized phenomenon (Heisenberg, 1971). Illuminating only a few ommatidia in a red-eyed fruit fly produces an ERG amplitude of a few mV, even at high light intensities (see **Fig. 9**). The ERG is usually recorded in a few varieties of white-eyed *Drosophila*. In physiological experiments, white-eyed mutants are often preferred because they lack the pupillary response, which in wild type are mediated by the movement of yellow pigment granules within the photoreceptors. Moreover, uniform »ganzfeld« illumination of the entire compound eye is easily achieved in the translucent retina of white-eyed mutants (Belusic, 2011). While the photoreceptor cells of the white-eyed mutants are otherwise physiologically unaffected, angular sensitivity of the photoreceptors in the white-eyed mutants is extended more than tenfold , so that image formation is heavily impaired. Thus, a white-eyed fly's ERG can exceed 40 mV peak-to-peak under bright illumination, with a sustained (DC) component of up to 30 mV (also see **Fig. 10**). This large amplitude results from the collective activity of numerous photoreceptors generating significant currents across the high-resistance basement membrane. The red screening pigment in the wild-type flies has an important role as a long-pass, red filter so that illuminations with broadband light allow long wavelength photons to reach the photoreceptors. These photons convert metarhodopsin to rhodopsin so that the metarhodopsin levels in the photoreceptors are kept sufficiently low to be manageable by the limited amount of arrestin molecules. In the white-eyed fruit flies, this is not the case. Under white light, the metarhodopsin levels in white eyes can become so high that the photoreceptors remain depolarized for long periods of time. Furthermore, in physiological experiments, short wavelength light is frequently used as a stimulus. White eyed flies then must be regularly exposed to orange or red light in order to interrupt any possible prolonged depolarizations.

More importantly, placement is crucial where advancing the measuring electrode into the retina such that it penetrates the basement membrane at approximately 120-150 μm

from the cornea, can be marked by a sudden 15 mV voltage drop and a change in ERG shape. At depths of 120-200 μm below the cornea, the receptor component becomes negligible, and neuronal transients dominate the ERG response. Lastly, there is emerging evidence that aging plays a significant role in the response of *Drosophila* to light stimulus (Kaladchibachi et al., 2022). Taken together, these observations suggest that there is a need to clearly evaluate outcomes in order to accurately interpret the ERG output observed in aging flies, as a function of GAL4-UAS system human gene insertion that we have addressed below.

2.1 Materials

MATERIALS

REAGENTS	DESCRIPTION	COMPANY & CATALOGUE #
100% Bleach Solution	Decontaminant (add catalogue number)	Clorox: USA001229
Normal Saline Solution (0.9%)	0.9 g of NaCl in 100 mL distilled water, mixed until salts dissolve	Fisher Chemical: S271-10
VU0155069	PLD1 Inhibitor	Tocris: 1781834-89-6
REAGENT SETUP	**IDENTIFIER**	**COMPANY**
Fly Stock 33799	RRID:BDSC_33799	Bloomington *Drosophila* Stock Center
Fly Stock 458	RRID:BDSC_50892	Bloomington *Drosophila* Stock Center
Fly Stock 32040	RRID:BDSC_32040	Bloomington *Drosophila* Stock Center

EQUIPMENT

NUMBER	EQUIPMENT	COMPANY & CATALOGUE #
1	Flaming/Brown Micropipette Puller	Sutter Instruments Company: P-97
2	W.F. 15X Eye piece	Narishige: MF-830 MicroForge
3	15mL High-Clarity Polypropylene Conical Tube	Falcon: 14-432-22
4	50mL Conical Centrifuge Tubes	ThermoFisher Scientific: 339650
5	Orthodontic Tray Wax	Kerr Lab: 8546850
6	Fire polished Borosilicate Glass with Filament	Sutter Instruments Company: BF150-110-10
7	ACE 1 Fiber Optic Light Source	Schott: A20500

8	Flowbuddy Flow Regulator	Flystuff: 59-122B
9	Stereo Microscope	Olympus: SZ51
10	Hook Up Wire, Solid, Type 18 Gauge, 100' Length, 300V, Red	NTE Electronics: WHS18-02-100
11	Disinfecting Bleach	Clorox: USA001229
12	Stereomicroscope	Wild: M5
13	Magnet Holder Base	Kanetec: MB-PB
14	S2 Amplifier	Kerr Scientific: 3000-521
15	16-Bit Acquisition System	Digidata 1322A Molecular Devices / Axon Instruments: 83029-1
16	Red film	Pangda: 4331997009
17	Aluminum Foil Roll	Fisherbrand: 01-213-100
18	Carbon Dioxide USP 50 LB	UTMB LINDE: CD M-50

GENERAL SUPPLIES

NUMBER	SUPPLIES
1	Paper Towels
2	Kimwipes
3	Gloves
4	Pens
5	Timer
6	Permanent Marker
7	Forceps
8	Scissors
9	Paint Brush
10	Fly Vials
11	Vial Plugs

DROSOPHILA FLY - FOOD MAKING PROTOCOL

Note: Mixer heat adjustment dial kept at "8"

INGREDIENTS - 3L OF FOOD	METHOD
Sugar - 37.05 g	1. Added first 3 ingredients to 3000 mL of dH_2O in mixing bowl
Yeast - 37.05 g	2. Mixer to speed “6” (much less than 5-10 mins to

	boil)
Jazz Mix - 467.22 g	3. Turned on heat. Heated to boiling, then shut off heat for the remainder of the protocol
Propionic Acid - About 24 mL	4. When food cooled to ~75° C, propionic acid was slowly added
dH_20	5. When food cooled to ~67° C, food was poured into vials
	6. 4 trays were immediately plugged and left at room temperature to set overnight
	7. Trays set well. One tray was placed in fridge and the other 3 trays were placed into the -20° C freezer

2.2. Methods

2.2.1 Preparation of Flies

- All *Drosophila* stocks were maintained at 25˚C on standard fly food under a 12:12-h light-dark cycle. *Drosophila* stocks were either purchased from Bloomington *Drosophila* Stock Center (BDSC), Bloomington, Indiana, USA or provided to us kindly by Dr. Paul Hardin, PhD (Texas A&M University, College Station, TX, USA) (CS, w^{1118}) or Dr. Raghu Padinjat, PhD (National Center for Biological Sciences, TIFR, Bangalore, INDIA). Flies enclosed from the cross were collected in fresh food vials and kept under standard conditions for 2 days for acclimatization.

2.2.2 Preparation of Electrodes

(1) Before starting the experiment, electrical wires must be prepared for recording via the electrodes. The PVC insulation from electrical wires (6-7 cm in length) is carefully removed, exposing the core. 4-5 such cores are put in a 15 mL centrifuge tube containing 100% bleach solution for 24 h. Core/wire turns dark brown after chloritization. Core is rinsed with water, dried and used for recording.

(2) Per fly, the experiment will require two electrodes, one to be placed on the eye, as the recording electrode, and one to be placed as a grounding electrode in the thorax.

(3) These will need to be prepared using the Flaming/Brown micropipette puller with the following microelectrode specifications and instrument settings:

- Microelectrode: BOROSILICATE GLASS with filament O.D.: 1.5mm, I.D.: 1.10mm, 10cm length.
- ITEM #: BF150-110-10
- Instrument settings:
  i. Ramp: 278
  ii. Program: 27
  iii. Pressure: 500
  iv. Heat: 289

v. Pull: 35
vi. Velocity: 49
vii. Time: 150

(4) The prepared electrodes are then placed in a petri dish with foam to ensure they do not break before usage. Any cracks seen in the electrode using the Narishige Microforge should warrant a new electrode being pulled and installed prior to any readings used.

(5) The electrodes are then filled with a 0.9% saline solution using a syringe. Once the solution is filled in the electrodes, they are then placed under a dissecting microscope (if using a non-filamentous glass capillary) or visual inspection microscope to evaluate the presence of bubbles. Any bubbles found must then be removed by gently tapping two fingers placed behind the electrode, to disturb the bubbles and have them float to the top.

(6) The electrodes are then placed in the ERG apparatus, with one within the recording arm and the other placed in grounding arm. The grounding wire needs to be connected to an insulated clip to a piece of metal to ensure it is grounded.

2.3 Placing Flies in Electrode

(1) Connect CO_2 tank to *Drosophila* CO_2 fly pads (Flystuff 59-114 Flystuff Flypad, CO_2 Anesthetizing Apparatus, Cat# 59-114), and then turn on gas.

(2) Using a *Drosophila* blow gun (Flystuff 54-104 Flystuff Blowgun, CO_2 Anesthesia Accessory, Cat# 54-104), CO_2 is passed into the test tube containing the flies, rendering them unconscious.

(3) Gently angle and tap the test tubes to transfer the flies to the CO_2 conduction plate, thus keeping them unconscious.

Note: the flies can only stay on the plate for a limited amount of time, so working fast to entrap the flies is critical as to not accidentally cause them to die of asphyxiation.

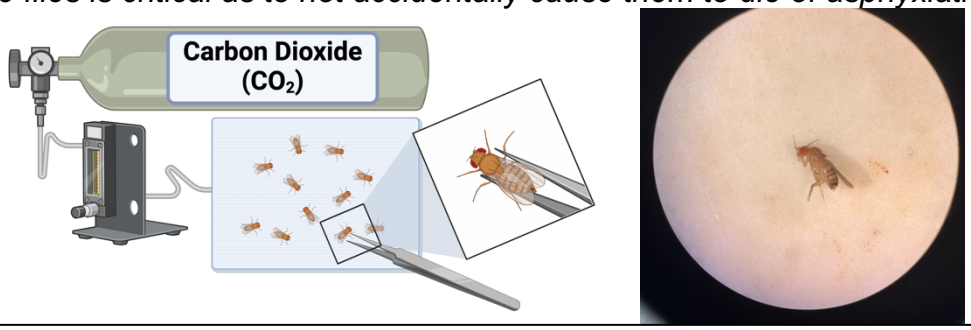

Figure 1: Pick up the fly using forceps and place on plate

(4) Using a razor blade, a 10 µL pipette tip is cut off 2-3 mm from the narrow end of the tip and discarded. Then measure 4mm down from the tip, and gently make another cut using the razor blade; this will leave an opening at both the bottom and top. The tip should be trimmed evenly to avoid uneven surfaces. This will allow passage of the fly from the larger opening and surfacing of its head and a small portion of the body through the smaller opening.

(5) Using a pair of tweezers, grab the target fly's wings and place the entire body through the larger opening. Slightly angle the cut in the plastic pipette such that the head of the fly would rest on the plastic lip of the cup pipette, but the back of the head was supported by the back of the plastic pipette (see **Fig. 2**).

(6) Then switch to a wax tipped needle and push the fly's body gently through the pipette, making sure the abdomen or the thorax is not damaged as this will kill the fly. As the head peaks out through the smaller opening, ensure some of the body can also be seen, as this part will be used to ground the fly.

Note: Leaving the hole too small will cause the fly to get compressed and die. Leaving it too large will cause the fly to either escape once it recovers consciousness or cause the fly to become pushed back into the pipette during the recording process. There is some trial and error associated with this, so some experimentation may be necessary to find the ideal length of the pipette tip.

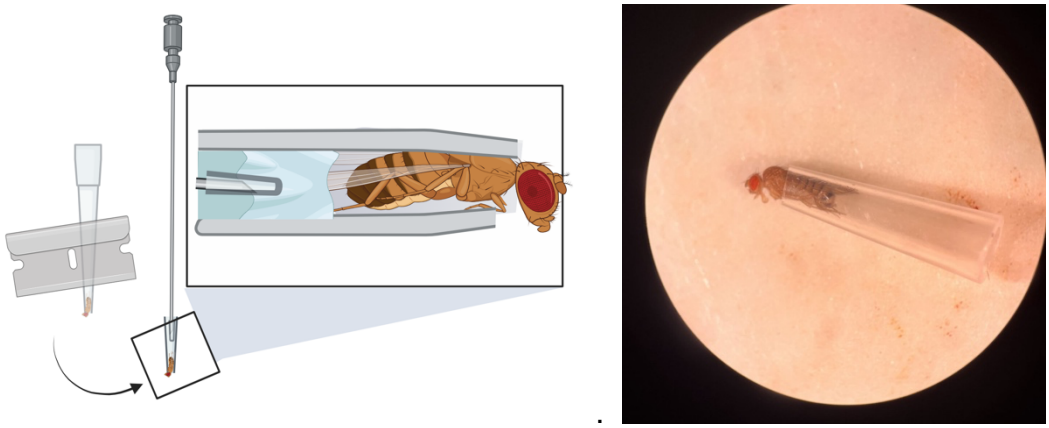

Figure 2: Place fly in pipette leaving some of the head and body exposed

(7) Secure the pipette tip in some wax that is adhered to a dish. The dish can then be turned upside down on the CO_2 plate to keep the fly unconscious for a little while longer, for about 30 seconds or so. This will keep the fly from escaping prematurely.

Note: for personal preference, when orienting the fly, we found higher success with securing it to the wax at an angle, so it looked like it was tipped over slightly. This makes it easier for the electrode to enter the body of the fly without breaking the electrode tip or the fly accidentally being pushed back into the pipette tip due to excess force.

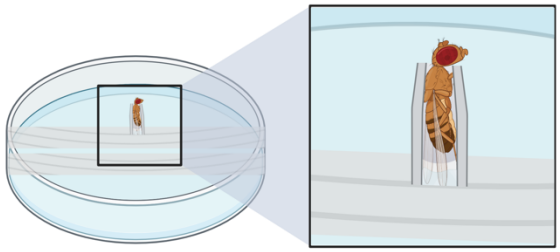

Figure 3: Orient pipette tip at an angle in a dish

(8) Carry the dish over to the ERG station carefully so as not to drop the dish or disturb the fly.

2.3 ERG Recording

(1) Sequentially, the Data Acquisition System, Amplifier and the computer are turned on. After the Amplifier is turned on (green light), the gain is set to 250x. Start the Clampex 8 software.

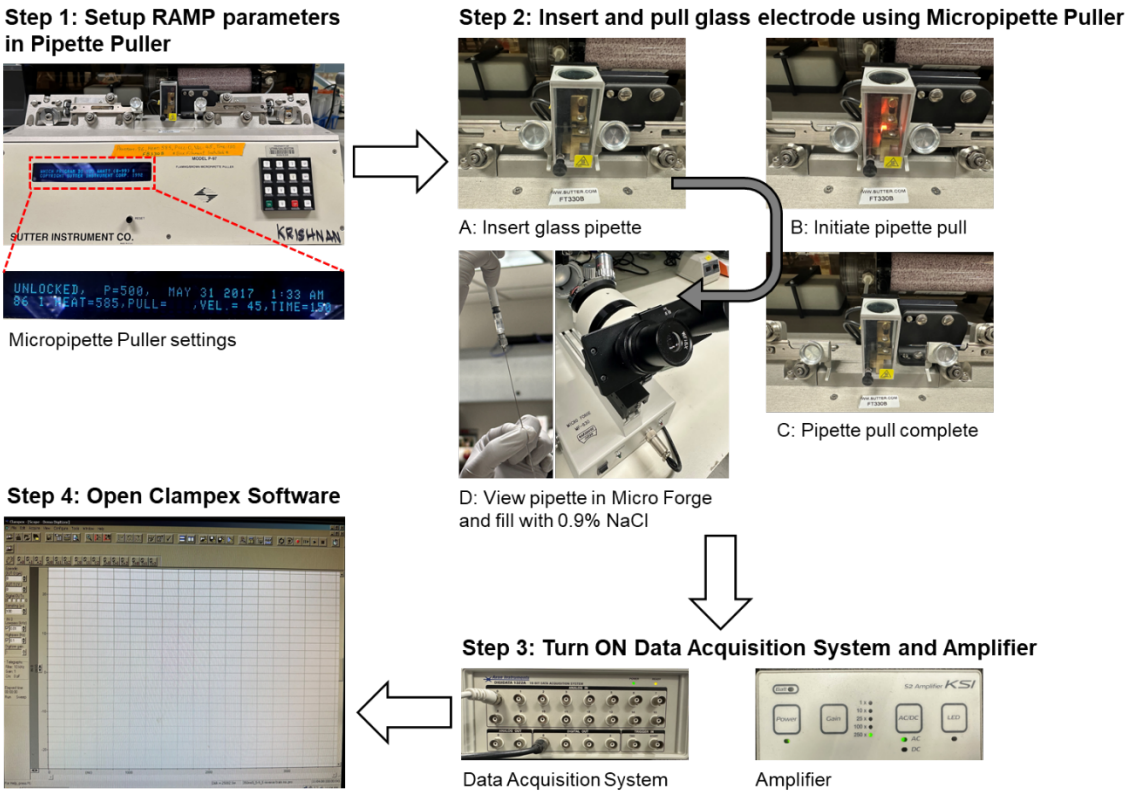

Figure 4: Pulling glass electrodes for ERG and setting up the Clampex program

(2) Once the fly has been placed on to the ERG station, check to see if it is still immobilized. It must not be moving out of the pipette tip, as this will make grounding much more difficult.

(3) Carefully start moving both electrodes towards the fly. Make sure they start at a high and far away enough distance, so the tips are not accidentally damaged. Any damaged electrode must be replaced, as this will create inaccurate readings.
(4) The recording electrode should be moved slightly above the fly's eye. The grounding electrode should be moved above the fly's thorax. Change the zoom on the microscope accordingly so that the tip can be visualized and oriented.

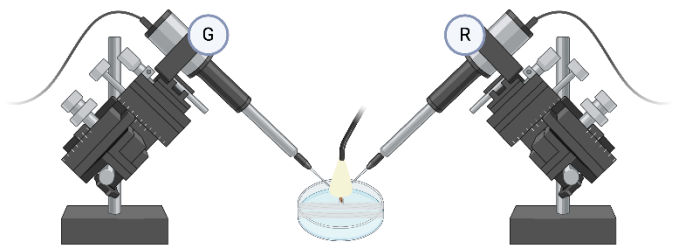

Figure 5: Run the ERG

(5) Lower the tip of the grounding electrode until it pierces the thorax. Lower the electrode slowly further into the body, observing for some reaction of the fly. Note: Make sure the electrode tip does not go through and touch the other side of the pipette, as this may damage the electrode or give inaccurate readings. Care is taken to slowly move the grounding electrode to prevent accidental death of fly. In any case the fly stops moving or dies in the process, all the steps are repeated with a fresh fly.
(6) Next, once the fly has been grounded, lower the recording electrode tip until the eye has been slightly indented. Take care not to accidentally pierce the fly's eye, as this will cause the eye to not register the light pulse.

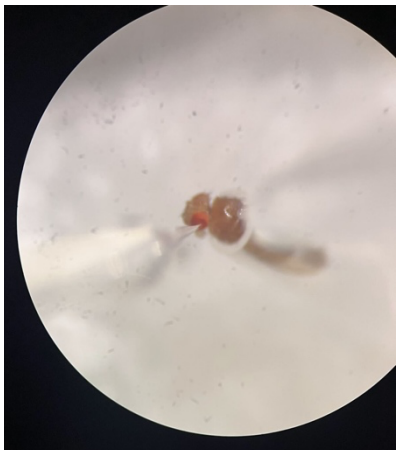

Figure 6: Be cautious when lowering the electrode towards the fly's eye

(7) A practice reading can be completed to make sure the right response from the fly is recorded, as below:

a. Then, a program will be run with 10 different light impulses, all of which will be repeated 10 times, for a total of 100 recordings. Each reading should look similar to the ones below:

b. Once the data is collected, the fly can be disposed, and the process can be repeated for each fly.

i. Note: the electrodes may dull between each fly and require replacement. If the amplitude of the recording drops, or if there is more noise in the trace, replace the glass pipettes and/or check chloridization of wires.

ii. If there is difficulty or resistance when attempting to ground the fly, replace the electrode and try again. This usually led to success for piercing the fly's body.

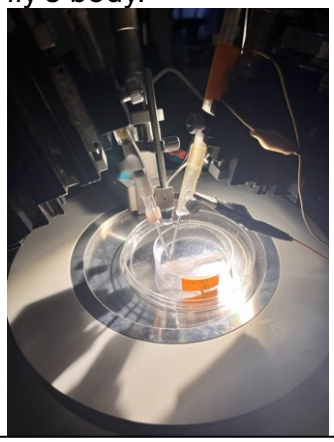

Figure 7: Experimental apparatus setup

Data Analysis

For each fly, we captured a sequence of recordings – 300 ms pulse, 500 ms pulse, 1000 ms pulse, 2000 ms pulse. These are captured at 5 pA, 10 pA, 15 pA, and 20 pA, respectively.

ERG recordings were collected in ABF files and opened using the software Clampfit (axon pCLAMP) 10.7. Canton-S Benzer (CS-BZ) represented in **Figure 8** shows the assessment of raw data that was adjusted to baseline to make the amplitude measurable between data sets. While the same approach was used for all the genotypes, there are obvious differences between the ERG traces that can be appreciated for CS (**Figure 8**) compared to w^{1118} (**Figure 9**) and a fly line generated by inserting the *UAS-hPLD1* (Panda et al., 2018; Thakur et al., 2016) in the w^{1118} background (**Figure 10**). The recordings have slight electrical interference noise as can

be seen by the minute, constant oscillations in recordings (panels A in each figure). This was likely due to these recordings being taken on the 10th floor of the research building. The noise was minimized using the “Electrical Interference Filter” feature to remove external harmonics (the after profile seen in panel B of each of the **Figures 8-10**). The nadir and peak are marked by cursors to determine the amplitude of the response. Upon transferring the values for the traces, and averaging the 10 traces, the values are used for the subsequent analyses. Panels D through M represent the different protocols that were used to assess the integrity of the neuronal response recorded from the different genotypes. From panels D->G, we assessed the effect of progressively stronger stimulus maintaining the same time of exposure while panels H->K, we assessed how the same intensity (5.5pA) when exposed for increasing time (500->2000ms) affected the three different components that we assessed in our study. Lastly, panels L and M were increasing and decreasing intensities (either 5.5->9.5 or vice versa respectively) for 350ms duration but without time to recover to see whether we observe changes in the three parameters of onset, receptor potential or offset amplitudes.

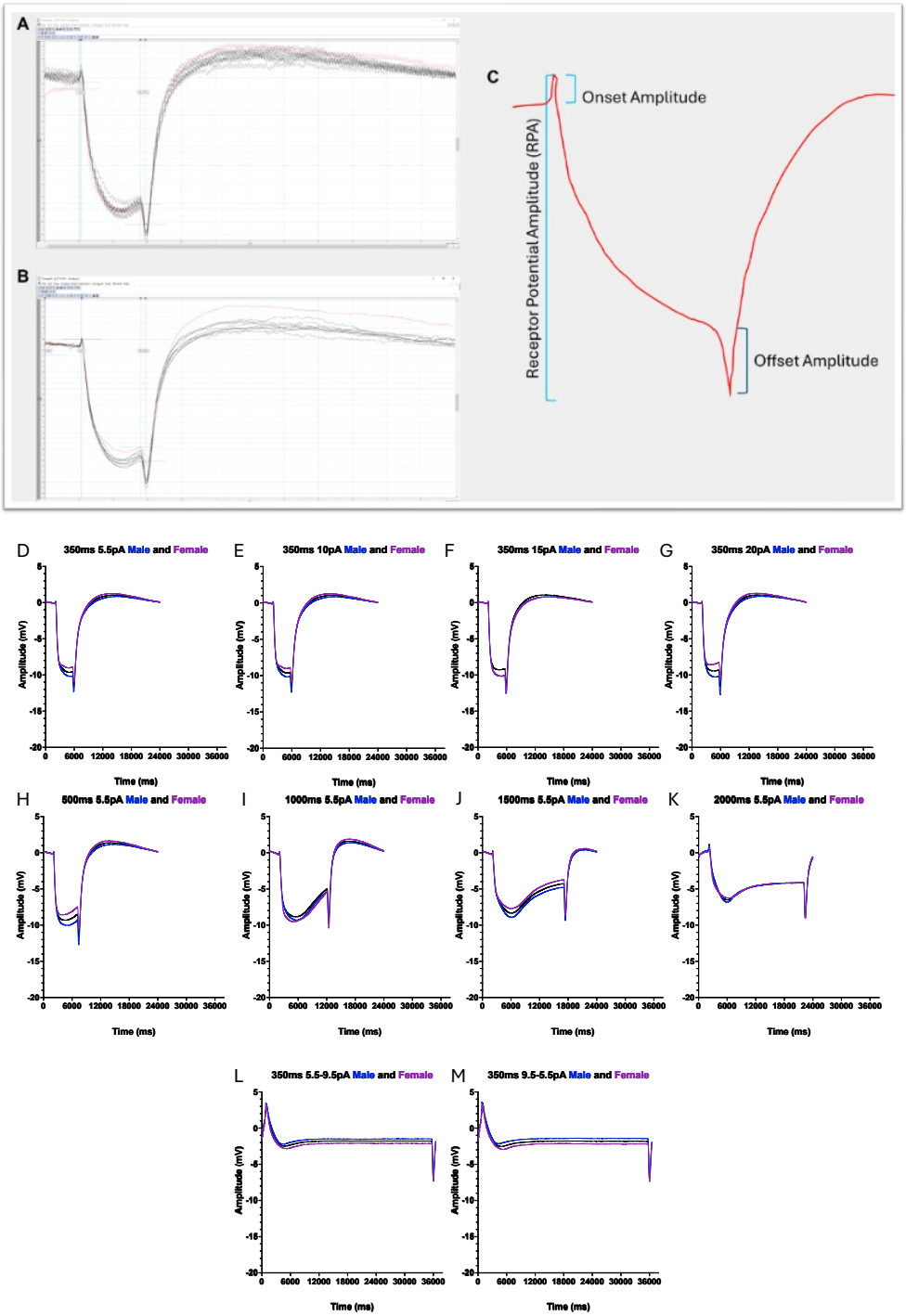

Figure 8: A represents the ERG with electrical interference, B represents the ERG with filtration of electrical interference (smoothening), C represents the overall hand drawn representation of the trace characteristics. D-M provides the traces for different stimulation intensities (top panels) at 350ms duration while the ERG patterns for increasing time durations at the same intensity (middle panels) are provided to illustrate the differences in onset, offset and receptor potential amplitude and ERG patterns observed for 350ms increasing or decreasing intensities (5.5-9.5 or 9.5 to 5.5pA, lower panels).

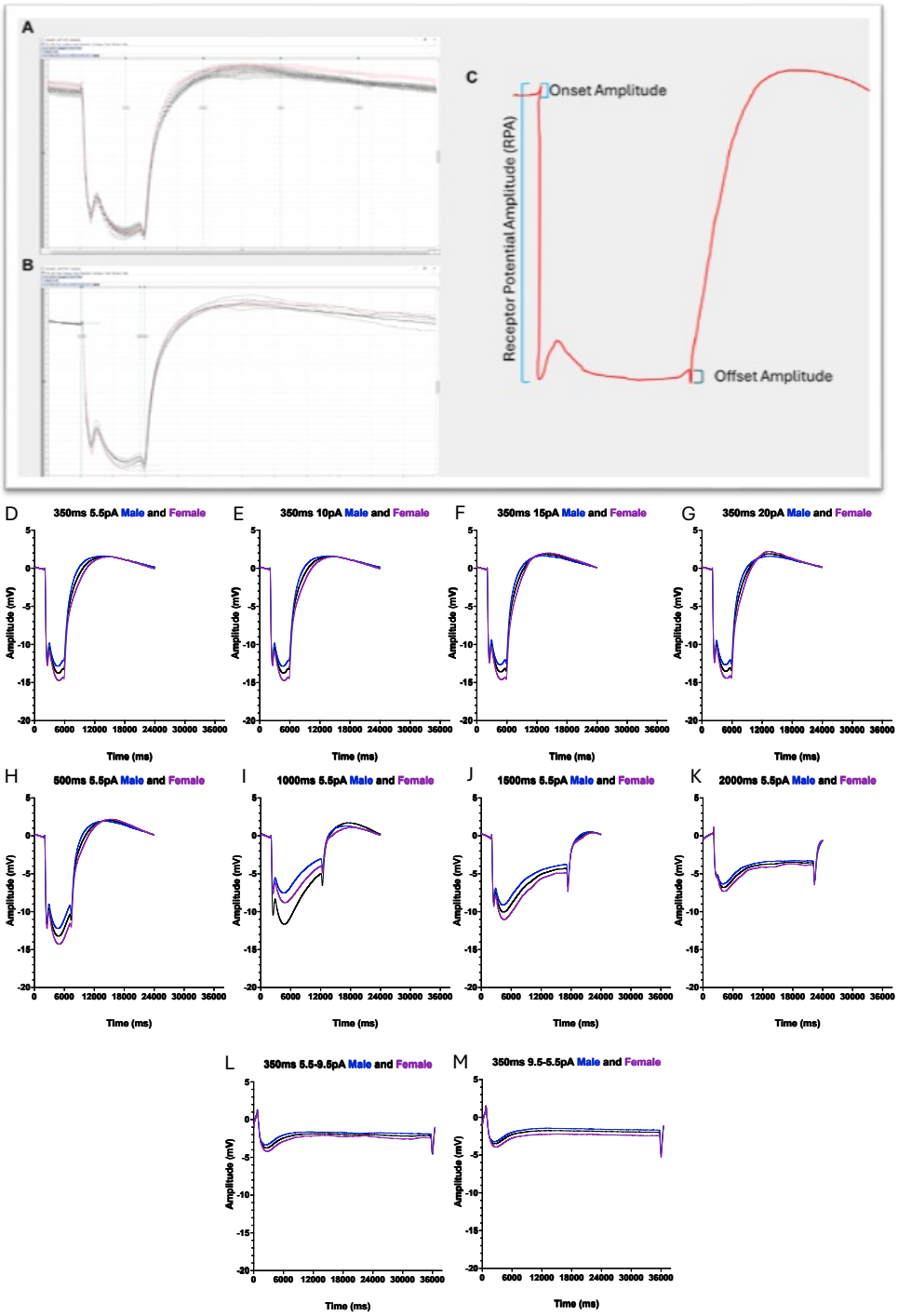

Figure 9: In the *w*^{1118} mutant group, there was a notable difference in ERG responses compared with the control (CS, Fig. 8) group. The overall amplitude was noted to be significantly greater in the *w*^{1118} group compared to the control, and that difference was consistent with all the tested durations. The offset amplitude in the *w*^{1118} group was minimized at shorter times as compasred to CS. It is important to note that at shorter times, the nadir was reached at shorter times.

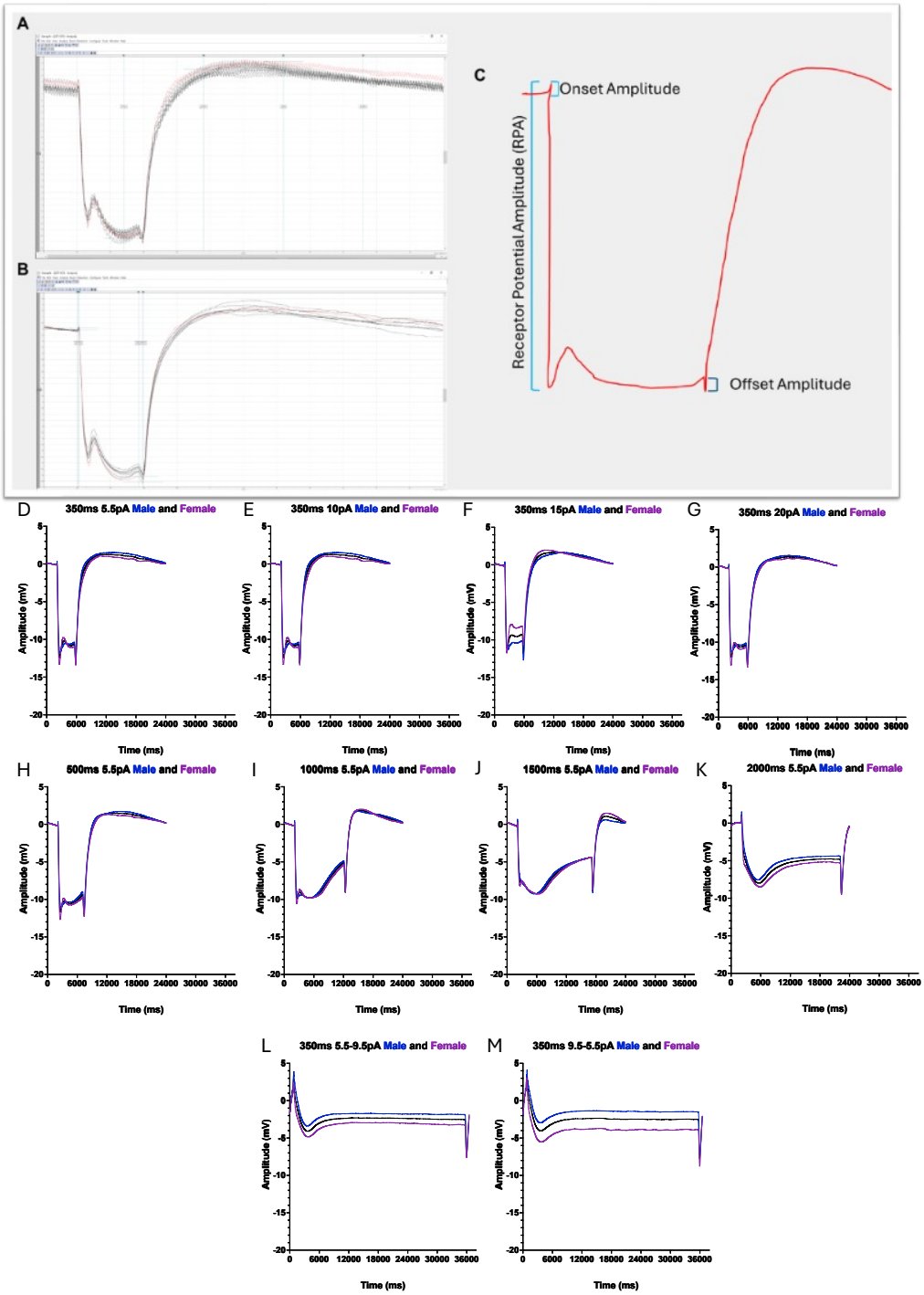

Figure 10: The w^{1118} ;+; *UAS-hPLD1*, shown above, presented with less pronounced onset and offset amplitudes than the w^{1118} group.

In the w^{1118} mutant group, there was a notable difference in ERG responses compared with CS. The overall RPA was significantly greater while the offset amplitude was compensated, resulting in a peak that was observed during the onset instead of a smooth transition to RPA as seen with the CS group. In the UAS-hPLD1 insertion into the w^{1118} background, where the construct expressed the mini white gene(Panda et al., 2018; Thakur et al., 2016), there is compensation in the genotype but not complete pigment restoration to CS levels which is reflected in the ERG responses (see **Fig. 11**). This white eye mutant combined with the human gene creates a slightly pigmented (red-orange) eye phenotype. The response curve followed a bimodal distribution, with the receptor potential peaking at 2 different instances before the offset amplitude was reached. These bimodal responses were relatively uniform at shorter time lengths and lower pA, and the response curved resembled the control group's response more so than the experimental group. At longer durations, the peaks became more pronounced, and the amplitude response was seen to be as great as the offset amplitude. The pronounced peaks may be hypothesized as a compensatory mechanism for visual reception (in the mutant flies). Such differences are important consideration to be incorporated into the observations when utilizing *Drosophila* as a translational model, especially when exploring the effect of human gene overexpression and its impacts on neurobiology.

3. Results:

This experiment compared three components of the ERG between groups: on-transient response, off-transient response, and the receptor potential amplitude. We compared the differences in responses between sexes and genotypes using a two-way ANOVA statistical test. Each group had 4-7 flies examined. Each stimulus was repeated 10 times every 20 seconds for each fly; the average of those 10 responses is reported here as the amplitude (mV) response of an individual fly for the assessed parameters. That average response was then combined with the averages of the other 4-7 flies in that group to create the final bar graph plotting amplitude as a function of intensity. These observations depict the differences that can be present in responses between sexes of the same genotype, and thus the importance in interpreting the effects with consideration and accounting for these differences, as illustrated below.

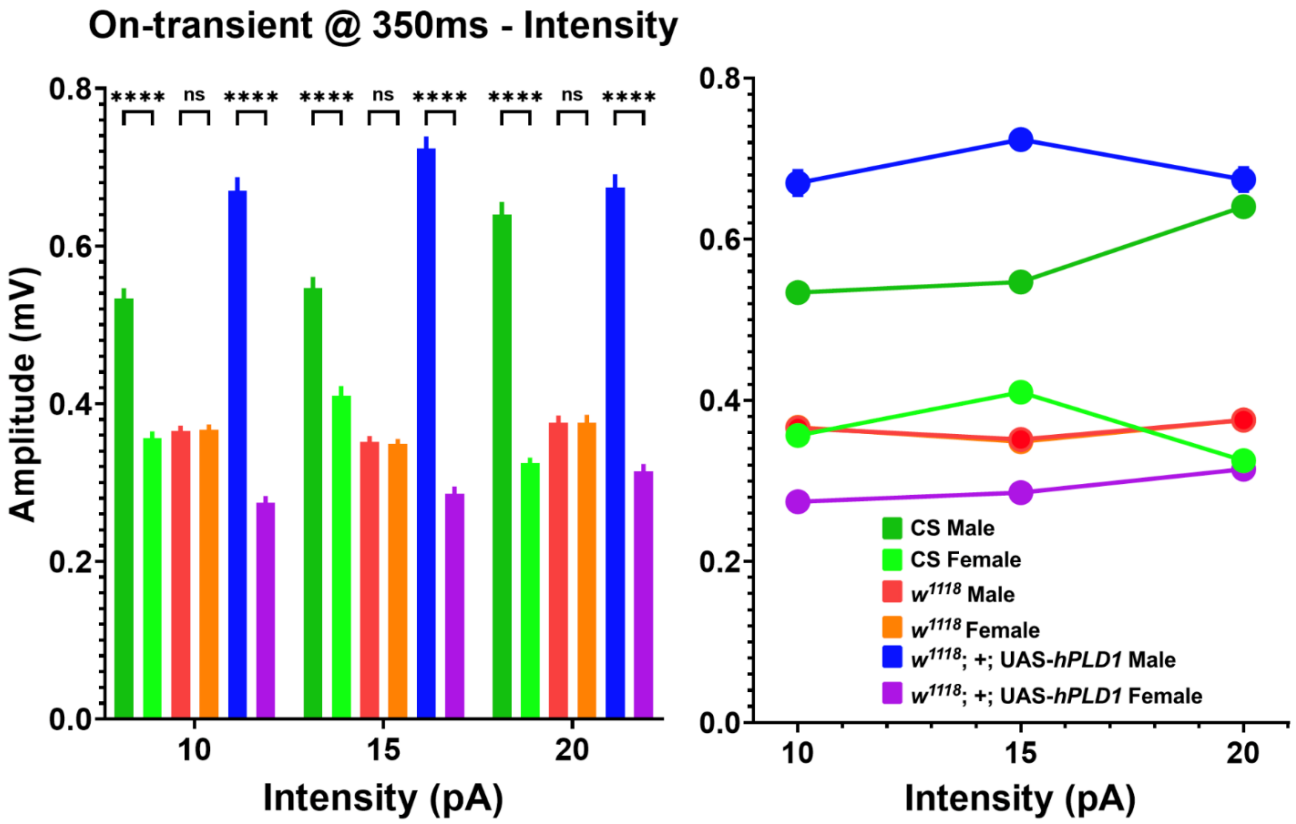

Figure 11: As the intensity increased, the trend seen was that the on-transient responses between sexes in the control group (green) and UAS-*hPLD1* group (blue/purple) were significant different. It can also be appreciated that there is a male/female response difference in the patterns. Alternatively, the mutant group sexes (red/orange) had identical responses as can be seen by their superimposed responses on the right. Repeated measures (mixed-effects model) 2-way ANOVA was performed with Sidak's multiple comparisons test with a single pooled variance. Details of the pairwise comparison provided as supplementary table.

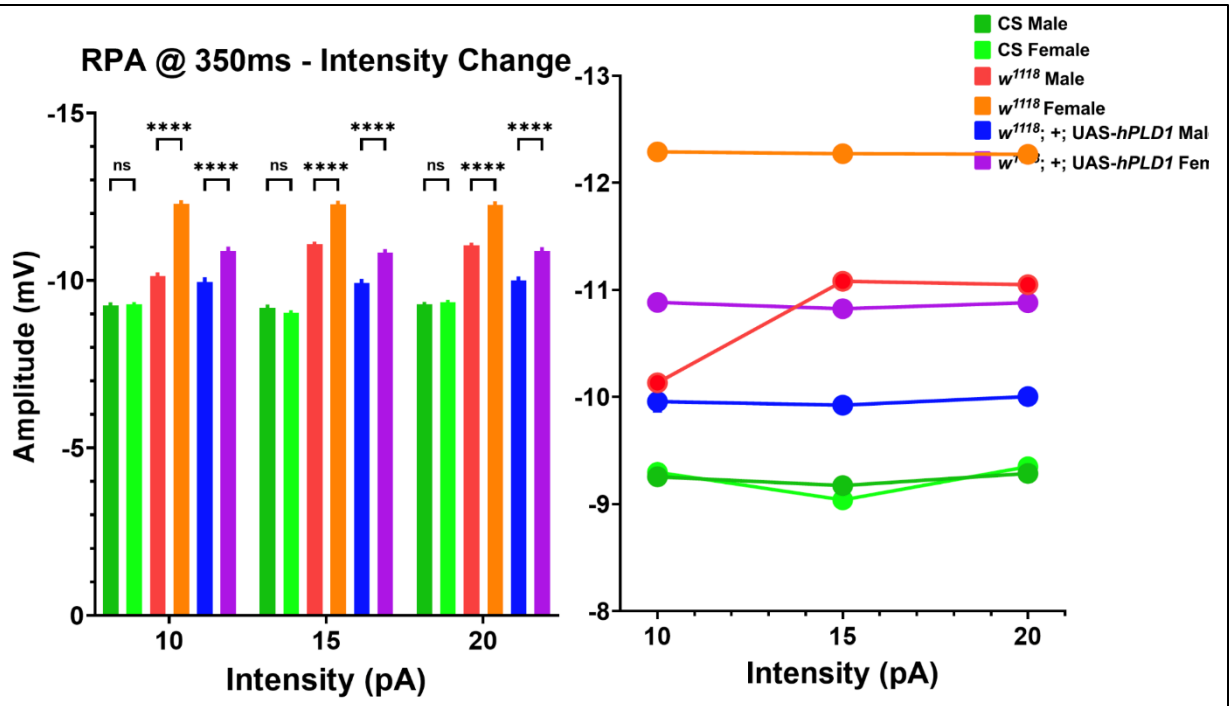

Figure 12: As the intensity increased, the trend seen was that the RPA response was significantly different between sexes for both the mutant and UAS-*hPLD1* genotypes, while the control group did not present any major changes between sexes. . Repeated measures (mixed-effects model) 2-way ANOVA was performed with Sidak's multiple comparisons test with a single pooled variance. Details of the pairwise comparison provided as supplementary table.

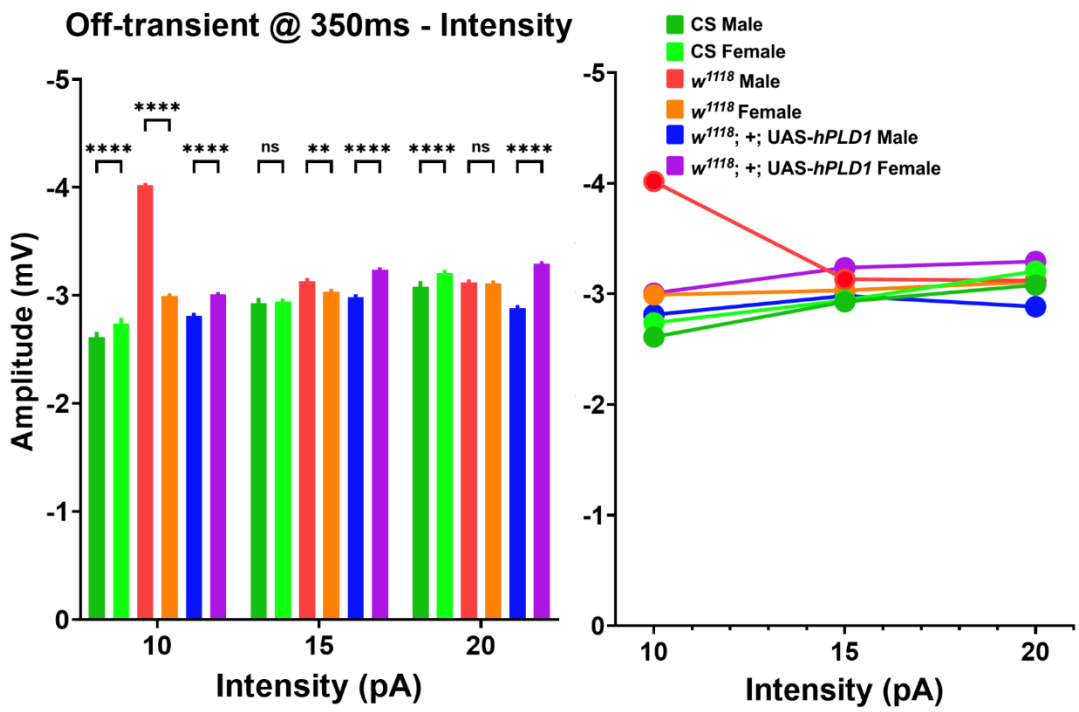

Figure 13: As the intensity increased, the trend seen was that the off-transient response was statistically different between sexes for both the mutant and UAS-*hPLD1* group at all tested intensity levels. Repeated measures (mixed-effects model) 2-way ANOVA was performed with Sidak's multiple comparisons test with a single pooled variance. Details of the pairwise comparison provided as supplementary table.

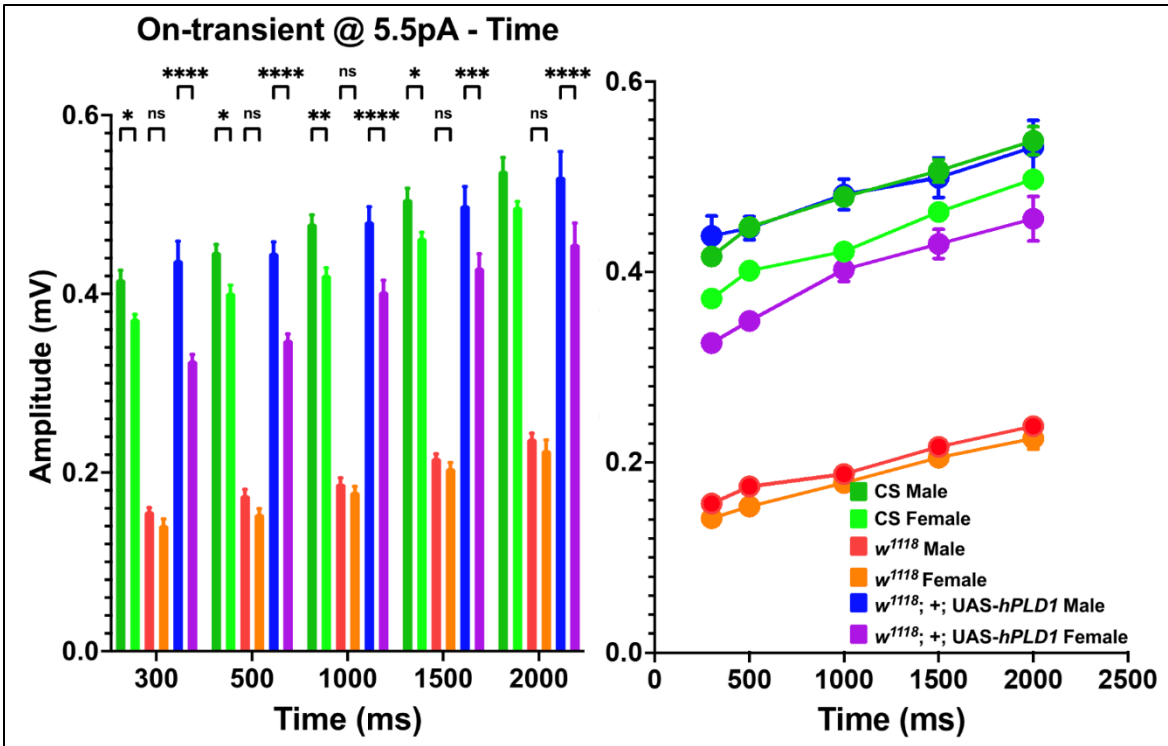

Figure 14: As the stimulus length increased with constant intensity, the trend seen was that the on-transient response was significantly different between sexes in the UAS-*hPLD1* group at all intervals. The responses were also different between the sexes in the control group at all intervals, though to a much smaller extent than the differences observed in the human gene group. The mutant gene did not significantly differ between sexes at any of the tested intervals. Repeated measures (mixed-effects model) 2-way ANOVA was performed with Sidak's multiple comparisons test with a single pooled variance. Details of the pairwise comparison provided as supplementary table.

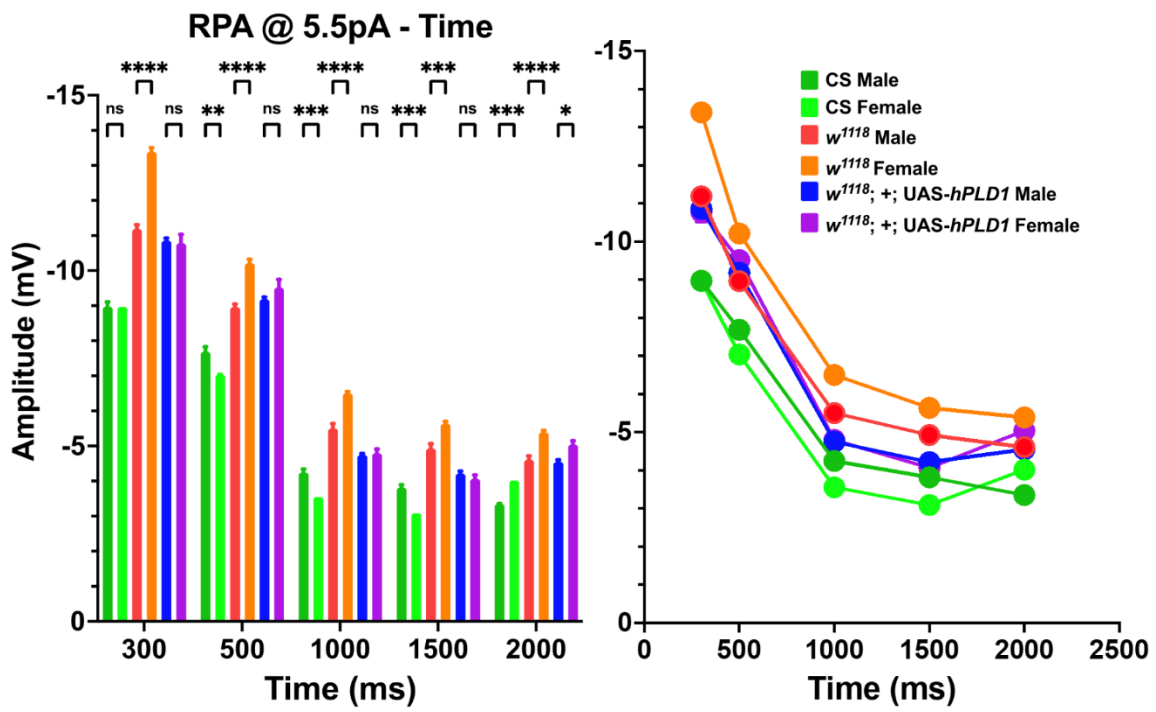

Figure 15: As the stimulus length increased with constant intensity, the trend seen was that the RPA was not significantly different in the UAS-*hPLD1* gene group at shorter intervals but was different between sexes at the longest tested interval (2000 ms). Repeated measures (mixed-effects model) 2-way ANOVA was performed with Sidak's multiple comparisons test with a single pooled variance. Details of the pairwise comparison provided as supplementary table.

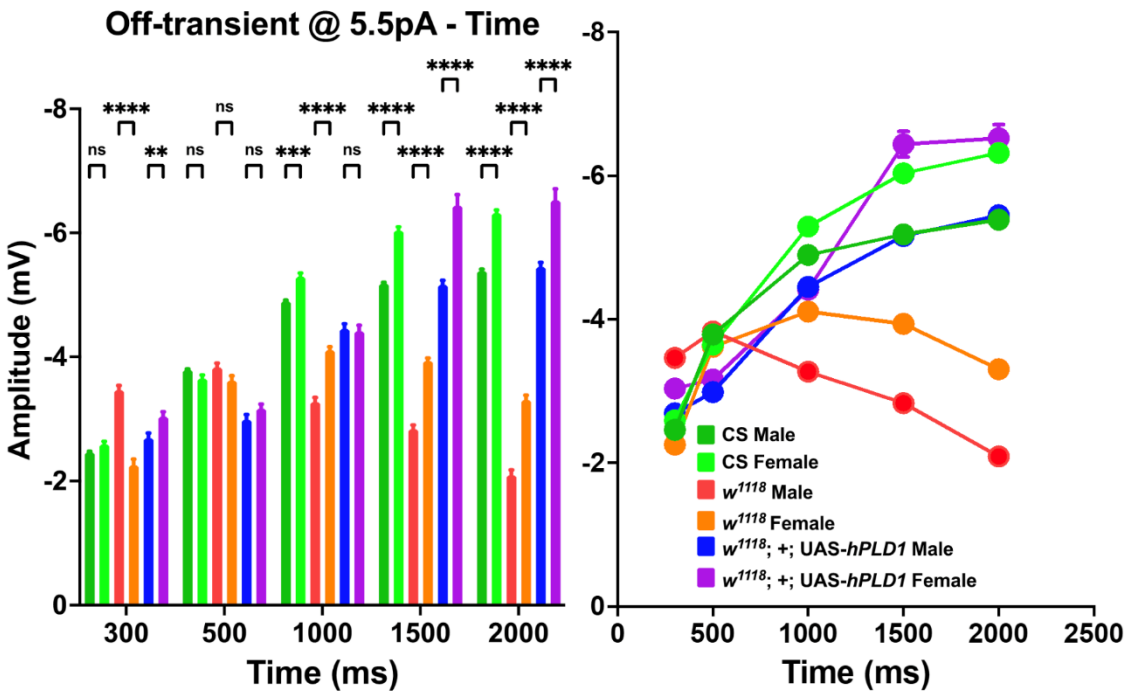

Figure 16: As the stimulus length increased with constant intensity, the trend seen was that the off transient became increasingly different between sexes in each group as the interval increased. Repeated measures (mixed-effects model) 2-way ANOVA was performed with Sidak's multiple comparisons test with a single pooled variance. Details of the pairwise comparison provided as supplementary table.

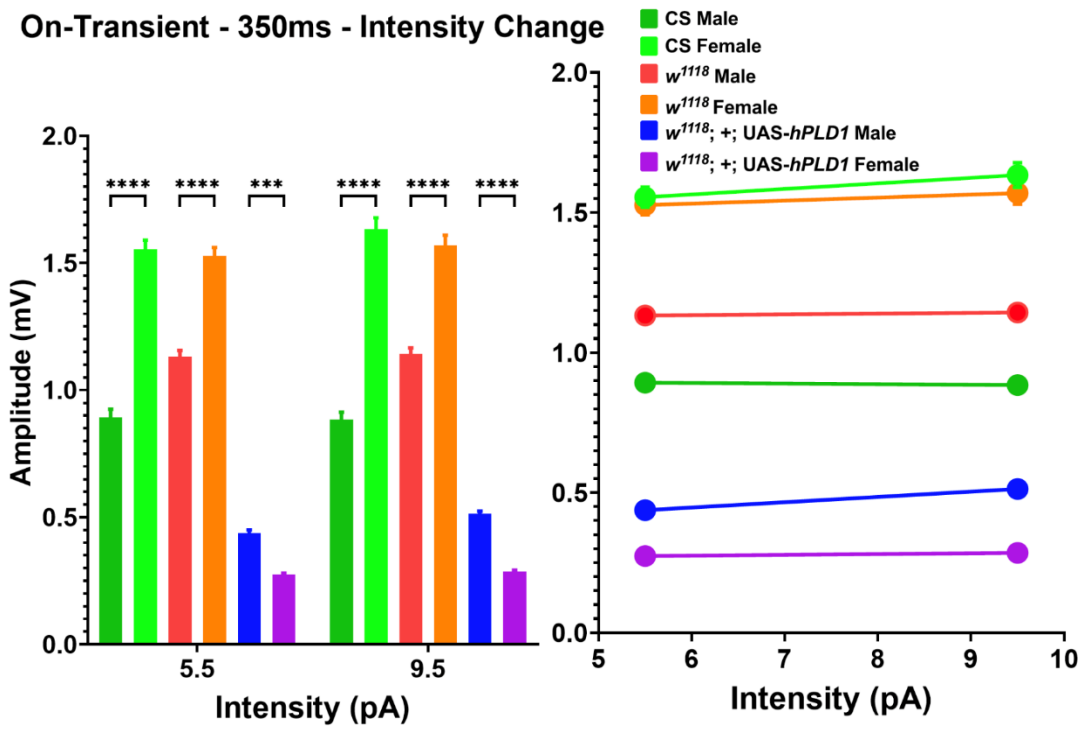

Figure 17: As the intensity increased (to a smaller extent than seen in figures 11-15) with constant interval, the trend seen was that the on-transient was significantly different between sexes in all groups at all tested intensity levels. Repeated measures (mixed-effects model) 2-way ANOVA was performed with Sidak's multiple comparisons test with a single pooled variance. Details of the pairwise comparison provided as supplementary table.

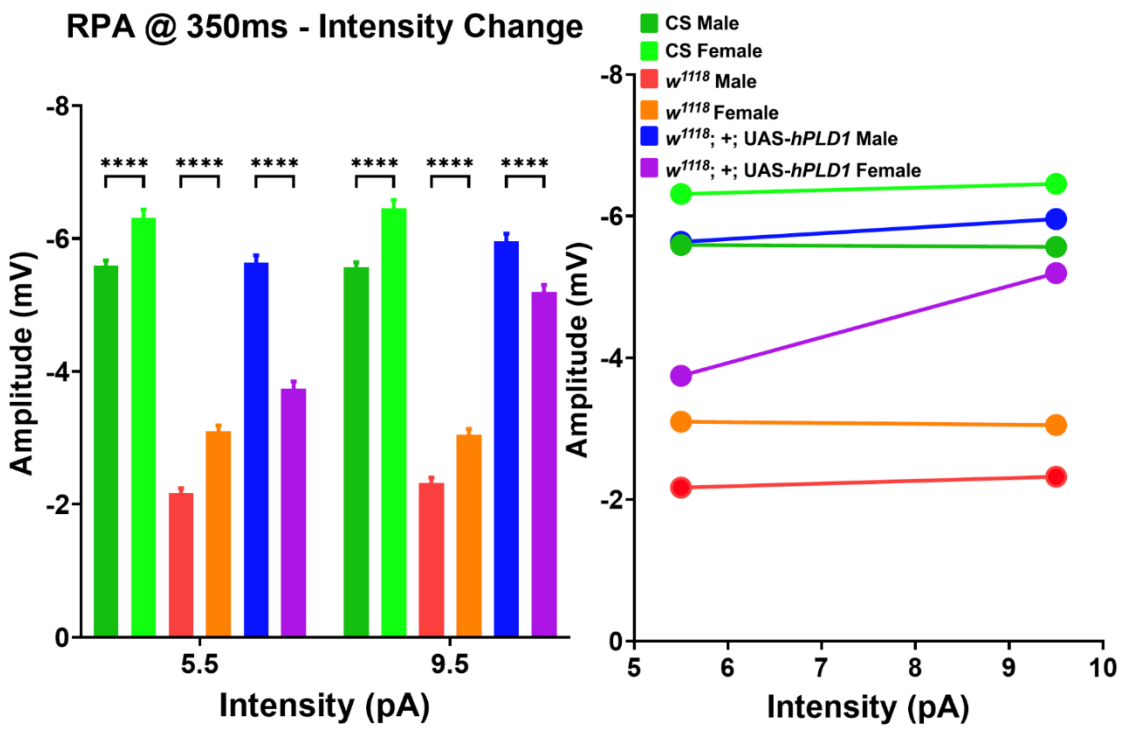

Figure 18: As the intensity increased (to a smaller extent than seen in previous figures 11-16) with constant interval, the trend seen was that the RPA was significantly different between sexes in all groups at all tested intensity levels. Repeated measures (mixed-effects model) 2-way ANOVA was performed with Sidak's multiple comparisons test with a single pooled variance. Details of the pairwise comparison provided as supplementary table.

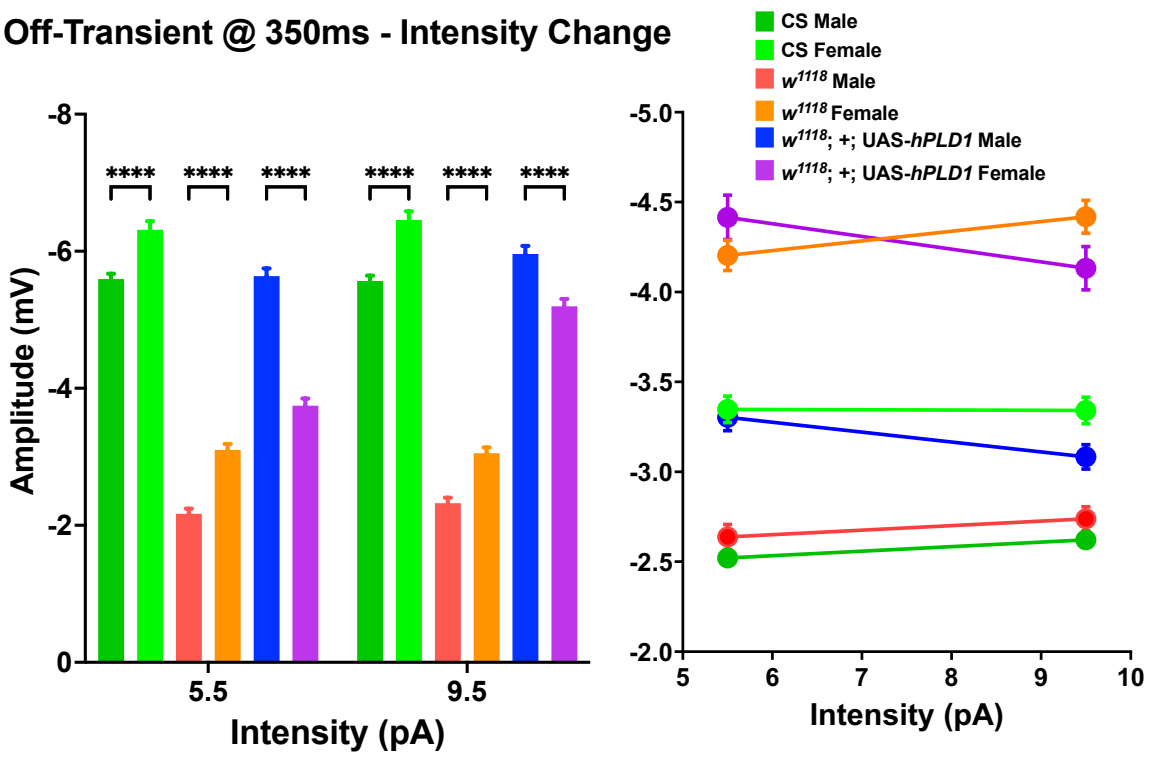

Figure 19: As the intensity increased (to a smaller extent than seen in figures 11-16) with constant interval, the trend seen was that the off-transient was significantly different between sexes in all groups at all tested intensity levels. Repeated measures (mixed-effects model) 2-way ANOVA was performed with Sidak's multiple comparisons test with a single pooled variance. Details of the pairwise comparison provided as supplementary table.

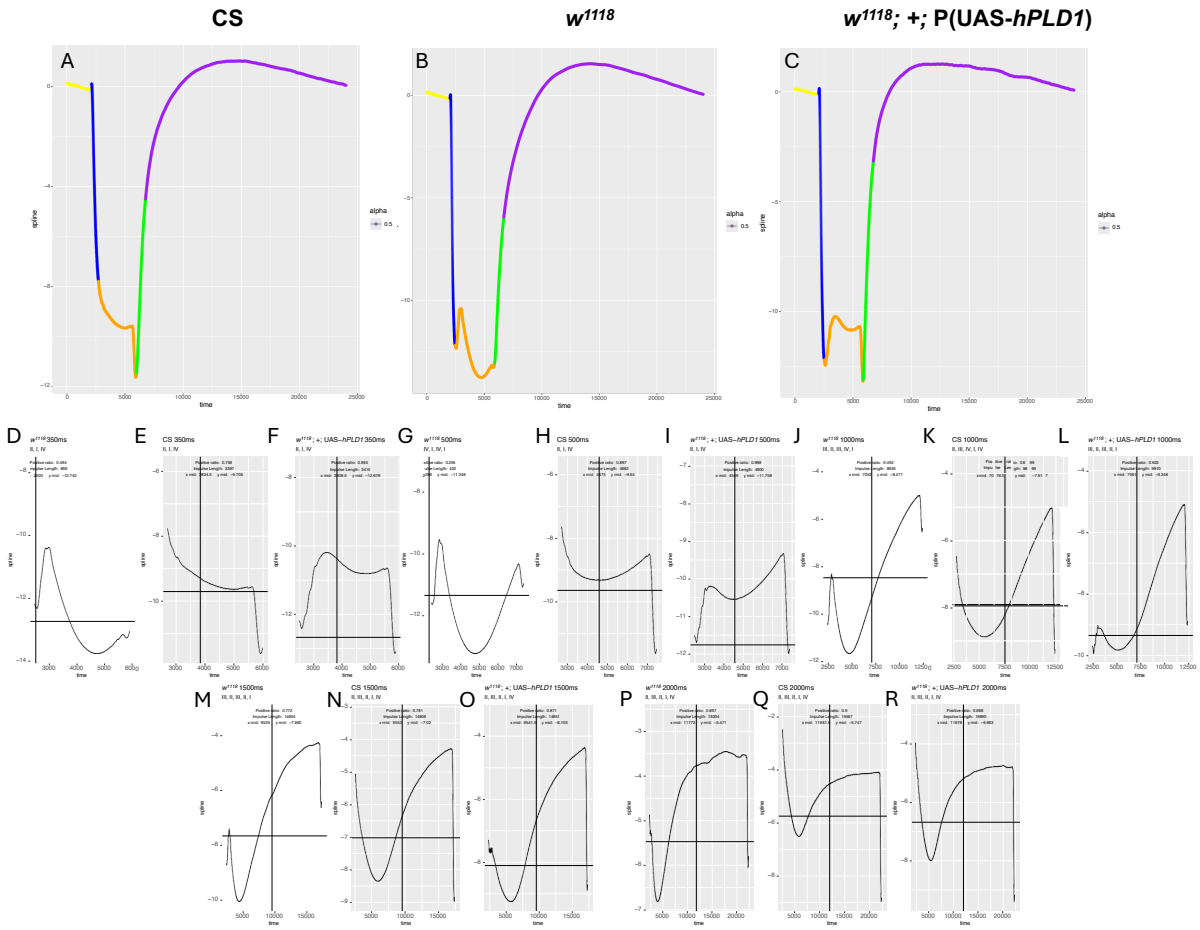

Figure 20: The average trace for 350ms pulse of light at 5.5pA and divided into regions to show the following profiles (see A, B and C). Regions in yellow show Pre-Impulse: all the points before the first one where the derivative is < -0.005. Blue Impulse is the Impulse-on-Drop: all the points where the derivative is < -0.005, before and including the one before first transition point back to derivative being >= -0.005. (There are spots later in the curve where the derivative may be small: but are not plotted here). Orange represents Mid-Impulse: all the points immediately after the first transition from derivative < -0.005 to >= -0.005 until right before the first point where the first derivative is > 0.005. Green is the Impulse Off Rise: all the points where the first derivative is > 0.005. Purple represents post-impulse: where all the points after the last drop recovers and where the first derivative is > 0.005. Panels D through R represent the expanded view of the orange part of the plots, or the Mid-Impulse. These were conducted to elucidate the nature of these unique patterns in more detail. We have centered the x-axis as halfway between the first peak in the On Drop, if there is one, otherwise the last peak in the Pre-Impulse, and the last peak before the last transition of the derivative from positive to negative within the Mid-Impulse. We have centered the y-axis at the halfway point between the y-value at the beginning of the Mid-Impulse and y-value of the last peak in the Mid-Impulse. The roman numerals for the different genotypes provide insight into the quadrants traversed by the traces (also see Table 1). At stimulation times 500ms and below, the 3rd quadrant is never visited by any of the genotypes in question. It is also interesting that here are more differences between CS and w1118 in the 500-1500 zone than at 350 or 2000, in terms of quadrants, but positive/negative ratios (the ratio of area under the curve in quadrants I and II to the area above the curve in quadrants II and IV) differ a lot at the lower end and are close at the top.

Stimulation (ms)	Quadrants	Genotype	Positive Area	Negative Area	Positive Ratio	Pulse Length	X Mid	Y Mid
350	II, I, IV	*w1118*	1517.26	1552.10	0.49	856.00	2500.00	-12.74
350	II, I, IV	CS	1233.88	393.21	0.76	3397.00	3834.50	-9.71
350	II, I, IV	*w1118;+;*P(UAS-*hPLD1*)	5976.91	33.41	0.99	3415.00	3808.50	-12.68
500	IV, I, IV, I	*w1118*	1326.71	3871.56	0.26	422.00	2286.00	-11.35
500	II, I, IV	CS	2798.89	322.84	0.90	4882.00	4575.00	-9.64
500	II, I, IV	*w1118;+;*P(UAS-*hPLD1*)	6938.68	16.41	1.00	4900.00	4549.00	-11.76
1000	III, II, III, IV, I	*w1118*	9535.81	9854.88	0.49	9936.00	7053.00	-8.48
1000	II, III, IV, I, IV	CS	7224.69	3107.74	0.70	9869.00	7076.50	-7.92
1000	III, II, III, II, I	*w1118;+;*P(UAS-*hPLD1*)	12811.81	1084.03	0.92	9910.00	7061.00	-9.35
1500	III, II, III, II, I	*w1118*	22987.66	6784.62	0.77	14854.00	9525.00	-7.66
1500	II, III, II, I, IV	CS	16139.95	4517.53	0.78	14806.00	9553.00	-7.02
1500	II, III, II, I, IV	*w1118;+;*P(UAS-*hPLD1*)	23214.23	3435.43	0.87	14851.00	9541.50	-8.10
2000	II, III, II, I, IV	*w1118*	25546.70	2933.38	0.90	19304.00	11772.00	-5.47
2000	II, III, II, I, IV	CS	20043.78	2230.91	0.90	19567.00	11981.50	-5.75
2000	II, III, II, I, IV	*w1118;+;*P(UAS-*hPLD1*)	23457.33	3575.62	0.87	19690.00	11978.00	-6.68

Table 1: Comparison of the genotypes measured using the quadrant profile associated with the peak of the RPA. When stimulation time (ms) when increased from 350 to 2000ms with a light intensity at 5.5pA, we were able to appreciate the following patterns. Except for 1000ms, the quadrant profile of the human PLD1 insert line parallels with CS, suggesting that the presence of pigmentation affects the RPA nadir characteristics. Given that there is a range of pigmentation reported with the P-element inserts depending on the location, this criteria may provide a quantification to stratify different UAS-lines based on the ERG responses as noted here. The positive to negative quadrants show variable ratios and are genotype dependent but also show correspondence with stimulation lengths suggesting multiple quantifiable metrics to further assess neuronal integrity. Additional parameters that we assessed include the pulse length, midpoint for X-axis and Y-axis that show patterns which can be quantified further.

Credit authorship contribution statement

NM: Data curation, Investigation, Methodology, Writing-original draft; MM: Data curation, Investigation, Methodology, Writing-original draft; AG: Data curation, Writing-original draft; SGS: Data curation, Investigation, Methodology, Writing-review and editing; DCJ: Data curation, Investigation, Software, Writing- review and editing; BK: Conceptualization, Data curation, Funding acquisition, Investigation, Methodology, Project administration, Resources, Software, Supervision, Writing – review and editing

Declaration of interests

The authors declare no competing interests.

Acknowledgements:

The authors would also like to acknowledge the Mitchell Center for Neurodegenerative Diseases for the common equipment provision. This work was supported by the Don and Nancy Mafrige Professorship in Neurodegenerative Diseases, Alzheimer's Association Research Grant (AARG-17-533363 B.K.), National Institutes of Aging (R21-AG059223 and R01-AG063945 B.K.).

References:

Belusic, G., 2011. ERG in Drosophila, in: Belusic, G. (Ed.), Electroretinograms. InTech, Rijeka, p. Ch. 12. https://doi.org/10.5772/21747

Heisenberg, M., 1971. Separation of receptor and lamina potentials in the electroretinogram of normal and mutant Drosophila. The Journal of experimental biology 55, 85–100. https://doi.org/10.1242/jeb.55.1.85

Kaladchibachi, S., Negelspach, D.C., Zeitzer, J.M., Fernandez, F.-X., 2022. Investigation of the aging clock's intermittent-light responses uncovers selective deficits to green millisecond flashes. Journal of Photochemistry and Photobiology B: Biology 228, 112389. https://doi.org/10.1016/j.jphotobiol.2022.112389

Panda, A., Thakur, R., Krishnan, H., Naik, A., Shinde, D., Raghu, P., 2018. Functional analysis of mammalian phospholipase D enzymes. Biosci Rep 38. https://doi.org/10.1042/BSR20181690

Thakur, R., Panda, A., Coessens, E., Raj, N., Yadav, S., Balakrishnan, S., Zhang, Q., Georgiev, P., Basak, B., Pasricha, R., Wakelam, M.J., Ktistakis, N.T., Raghu, P., 2016. Phospholipase D activity couples plasma membrane endocytosis with retromer dependent recycling. Elife 5, e18515. https://doi.org/10.7554/eLife.18515